Study of $B^0 \to K^{*0}\tau\tau$ at FCC-ee

Tristan Miralles - FCC Clermont group

FCC Physics Workshop Kraków: 26^{th} of January

- Third generation couplings in quark transitions are the less-well known.
- Specific models addressing the Flavour problem(s) often provide $b \to \tau$ enhancements or modifications w.r.t. the SM $\Rightarrow$ $b \to s\tau\tau$ ($m_\tau \sim 20 m_\mu$) is a must do to sort out the BSM models. Problem : measuring the ν's.
- Thanks to its clear experimental environment and its ability to produce boosted b-hadrons, FCC-*ee* looks like the right place to reconstruct the ν's.
- SM : the $b \to s\tau\tau$ transition proceeds through an electroweak penguin diagram.
- Study of the rare heavy-flavoured decay $B^0 \to K^*\tau^+\tau^-$ at FCC-*ee*[1]. SM prediction : BR=$\mathcal{O}(10^{-7})$ $\to$ not observed yet (present limit : $\mathcal{O}(10^{-3} - 10^{-4})$ [2]).

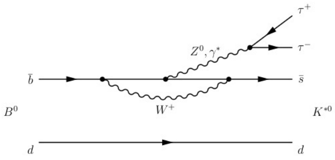

Figure – EW penguin quark-level transition

- The $B^0 \rightarrow K^*\tau\tau$ decay topology is driven by the tau decay multiplicity.
- There are from 2 to 4 neutrinos (not detected) and at least 4 charged particles in the final state and one, two or three decay vertices.
- We focus on the 3-prongs tau decays ($\tau \rightarrow \pi\pi\pi\nu$) for which the decay vertex can be reconstructed in order to solve fully the kinematics.
- 10 particles in the final state ($K, 7\pi, \nu, \bar{\nu}$), 3 decay vertices and 2 undetected neutrinos.

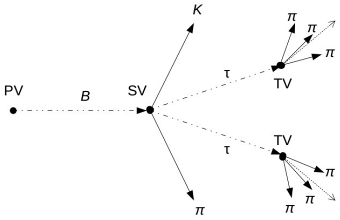

Figure – Decay topology

Goal : explore the feasibility of the search for $B^0 \rightarrow K^*\tau^+\tau^-$ and give the corresponding detector requirements.

- The events used in this work are generated with Pythia [3] ($Z \to b\bar{b}$ and hadronisation) and EvtGen [4] (forcing the decay with adequate models).
- 100000 events were generated for the decay thanks to the sw team Clement, Donal and Emmanuel.
- The reconstruction is performed with the FCC Analyses sw using Delphes [5] simulation (featuring the IDEA [6] detector).
- The simulated data use particles reconstructed with the momentum resolution given by the IDEA drift chamber tracking system. One of the goal of the study is to address the required vertex reconstruction precision hence the vertex resolution is emulated.
- Uproot is used in this analysis $\to$ thanks to Jim Pivarski for his reactivity with the development.

- To fully reconstruct the kinematics of the decay $\rightarrow$ neutrinos momentum are needed.
- Enough constraints are available in order to determine the missing coordinates.
- Energy momentum conservation at τ decay vertex $\Rightarrow$ gives the neutrino momentum at the cost of a quadratic ambiguity :

$$\begin{cases} p^{\perp}_{\nu_\tau} = -p^{\perp}_{\pi_t} \\ p^{\parallel}_{\nu_\tau} = \dfrac{((m_\tau^2 - m_{\pi_t}^2) - 2p_{\pi_t}^{\perp,2})}{2(p_{\pi_t}^{\perp,2} + m_{\pi_t}^2)}.p^{\parallel}_{\pi_t} \pm \dfrac{\sqrt{(m_\tau^2 - m_{\pi_t}^2)^2 - 4m_\tau^2 p_{\pi_t}^{\perp,2}}}{2(p_{\pi_t}^{\perp,2} + m_{\pi_t}^2)}.E_{\pi_t} \end{cases}$$

- A selection rule has to be build in order to solve the ambiguities.
- Practically energy-momentum conservation at the B decay vertex gives a condition between τ's and K^* :

$$p_{\tau^+_-} = -\frac{\vec{p}^{\perp}_{K*}.\vec{e}_{\tau^+_-}}{1-(\vec{e}_{\tau^+_-}.\vec{e}_B)^2} - p_{\tau^-_+}.\frac{\vec{e}_{\tau^+_-}.\vec{e}_{\tau^-_+} - (\vec{e}_{\tau^+_-}.\vec{e}_B)(\vec{e}_{\tau^-_+}.\vec{e}_B)}{1-(\vec{e}_{\tau^+_-}.\vec{e}_B)^2}$$

- Vertex resolution is introduced by Gaussian smearings.
- PV : 3D normal law of 3 µm width (conservatively, does not limit the method).
- SV & TV $\rightarrow$ ellipsoidal (decaying particle direction as reference) :
  - longitudinal,
  - transverse.
- Investigate the impact of the resolution on the B^0 invariant-mass reconstruction.
- Several working points examined (longitudinal-transverse configuration).

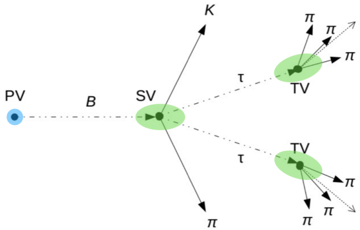

$\Rightarrow$ investigate vertices resolution impact on the feasibility of the observation of $B^0 \rightarrow K^* \tau^+ \tau^-$.

From previous talks (Paris)

- The vertex resolution drives the feasibility of this measurement :
  - Secondary and tertiary vertices $\rightarrow$ main drivers of the reconstruction,
  - Primary vertex resolution has an impact on the selection rule.
- 20-3µm (longitudinal-transverse) yield prediction [i] : $\mathcal{N}_{K^*\tau\tau\rightarrow K7\pi2\nu} \approx 184 \pm 24$.
- Reconstruction method has been validated with simulated signal events and provided the building blocks of the resolution performance.

i. Detailed in appendix.
ii. The 6 dominant backgrounds (in terms of visible BF and number of additional missing particle) are generated.

From previous talks (Paris)

- The vertex resolution drives the feasibility of this measurement :
  - Secondary and tertiary vertices $\rightarrow$ main drivers of the reconstruction,
  - Primary vertex resolution has an impact on the selection rule.
- 20-3µm (longitudinal-transverse) yield prediction [i] :
  $\mathcal{N}_{K^*\tau\tau\rightarrow K7\pi2\nu} \approx 184 \pm 24$.
- Reconstruction method has been validated with simulated signal events and provided the building blocks of the resolution performance.

- Several vertex resolution configurations have been used, in the following 20-3µm resolution will be used as a guide.
- The next step is to identify the dominant backgrounds and quantify their contribution [7] in order to establish the feasibility of the measurement.
- Relevant backgrounds are the ones with a similar final state [ii] ($K7\pi$).
- A summary of possible backgrounds (visible BF and missing particles) follows.

i. Detailed in appendix.
ii. The 6 dominant backgrounds (in terms of visible BF and number of additional missing particle) are generated.

Backgrounds identification

Decay	BF (SM/meas.)	Intermediate decay	BF_had	Additional missing particles
Signal : $B^0 \to K^*\tau\tau$	1.30×10^{-7}	$\tau \to \pi\pi\pi\nu$, $K^* \to K\pi$	9.57×10^{-11}	
Backgrounds $b \to c\bar{c}s$:				
$B^0 \to K^{*0}D_sD_s$	2.78×10^{-4}	$D_s \to \tau\nu$ [iii]	5.79×10^{-10}	2ν [iv]
		$D_s \to \tau\nu, \pi\pi\pi\pi^0$ [iii] [v]	6.52×10^{-10}	ν , π^0
		$D_s \to \pi\pi\pi\pi^0$ [iii] [v]	7.35×10^{-10}	$2\pi^0$,
		$D_s \to \pi\pi\pi 2\pi^0$ [iii] [v] [vi] [vii]	5.17×10^{-8}	$4\pi^0$,
$B^0 \to K^{*0}D_sD_s^*$	8.78×10^{-4}	$D_s \to \tau\nu$ [iii]	1.83×10^{-9}	2ν, γ/π^0
		$D_s \to \tau\nu, \pi\pi\pi\pi^0$	2.06×10^{-9}	ν , π^0, γ/π^0
		$D_s \to \pi\pi\pi\pi^0$	2.32×10^{-9}	$2\pi^0$, γ/π^0
$B^0 \to K^{*0}D_s^*D_s^*$	9.10×10^{-4}	$D_s \to \tau\nu$	1.90×10^{-9}	2ν, $2\gamma/\pi^0$
		$D_s \to \tau\nu, \pi\pi\pi\pi^0$	2.14×10^{-9}	ν , π^0, $2\gamma/\pi^0$
		$D_s \to \pi\pi\pi\pi^0$	2.41×10^{-9}	$2\pi^0$, $2\gamma/\pi^0$
Backgrounds $b \to c\tau\nu$:				
$B_s \to K^{*0}D\tau\nu$	1.44×10^{-4}	$D \to \pi\pi\pi\pi^0$	3.28×10^{-9}	ν, π^0
$B_s \to K^{*0}D^*\tau\nu$	3.16×10^{-4}	$D^* \to D^0\pi, D\pi^0$		
		$D \to \pi\pi\pi\pi^0$	2.21×10^{-9}	ν, $2\pi^0$
		$D^0 \to 2\pi 2\pi\pi^0$	1.76×10^{-9}	ν, $2\pi^0$, $2\pi^\pm$
$B^0 \to K^{*0}D_s\tau\nu$	9.40×10^{-6}	$D_s \to \tau\nu$ [iii]	3.68×10^{-10}	2ν [iv]
		$D_s \to \pi\pi\pi\pi^0$	4.15×10^{-10}	ν, π^0
$B^0 \to K^{*0}D_s^*\tau\nu$	2.06×10^{-5}	$D_s \to \tau\nu$	8.07×10^{-10}	2ν, γ/π^0
		$D_s \to \pi\pi\pi\pi^0$	9.09×10^{-10}	ν, π^0, γ/π^0

iii. The generated backgrounds.
iv. Not totally irreducible due to additional missing neutrinos or lifetimes.
v. $D_s \to 3\pi n\pi^0$ modes involves η/ω intermediate states (see appendix).
vi. Displayed once but can be considered for each $D_s \to \pi\pi\pi\pi^0$.
vii. Background with the biggest BF, very dangerous if not killed by the reconstruction.

Selection rule behaviour and landscape with background

- Selection rule → select preferentially peaking solutions for the background.
- FCC week status was : $D_s \to \pi\pi\pi\pi^0\pi^0$ is overwhelming.
- The capability to identify the π^0 from one η/ω allows to reduce this background.
- The probability for an event to survive is : $(1-\epsilon_{\pi^0})^2$, ϵ_{π^0} is the probability to identify one π^0.
- With $\epsilon_{\pi^0} = 0.8$ $D_s \to \pi\pi\pi\pi^0\pi^0$ is clearly reduced but still large.
- Additional selection is required. We played a Multivariate selection (XGBoost [8]).

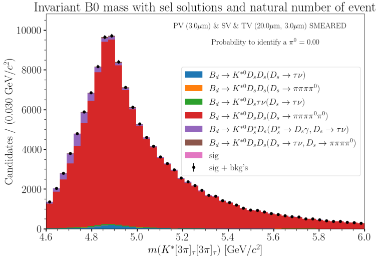

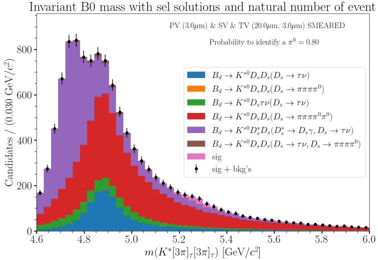

How to deal with $D_s \to \pi\pi\pi\pi^0\pi^0$

- To clean further the backgrounds (and mostly $D_s \to 3\pi 2\pi^0$) a preselection is applied.
- Among the avaible variables it appears that the "Dalitz plane" built on the invariant mass of the two neutral couples of $\pi^+\pi^-$ from τ candidates is discriminative.
- Rank the two invariant masses and display the plane (minimum vs maximum $m_{\pi^+\pi^-}$). Signal (top) and $D_s \to \pi\pi\pi\pi^0\pi^0$ (bottom).

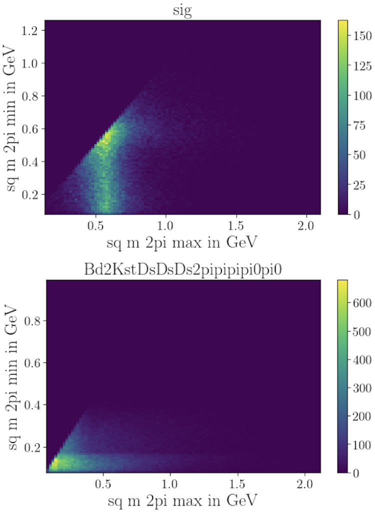

Preselection

- The preselection has been built on to the available variables (including those Dalitz plane ones).
- The picture show a first improvement.
- In addition, $D_s \to \pi\pi\pi\pi^0\pi^0$ is no more overwhelming.
- The MVA could now be built to fight several types of background on the [5,5.6] GeV mass window.

Variable	Cut
$m^2_{2\pi\,min}$ & $m^2_{2\pi\,max}$	<0.3 & <0.5 GeV
p_{K*}	<1GeV
$p_{3\pi}$	<1GeV
$p_{\pi\,max}$	<0.25GeV
$p_{\pi\,min}$	<0.2GeV
FD_B	<0.3mm
FD_τ	>4mm
$m_{3\pi}$	<0.750GeV
$m_{2\pi\,max}$	<0.5GeV
$m_{2\pi\,min}$	>1GeV

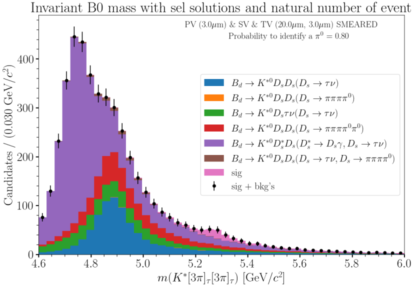

- Dataset generated with signal and the collection of available backgrounds.
- The backgrounds are considered in natural proportion (after the preselection).
- 50/50 split train/validation.
- Previous variables are given as inputs as well as the reconstructed p_τ of each τ candidate.
- Parameters from a simple optimisation (based on AUC) : learning rate=0.01, max depth=2 and number of trees=1000.
- Overtraining plot in order to check the validity of the training $\rightarrow$ OK.

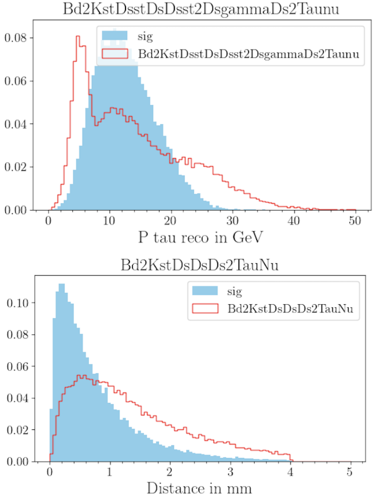

Figure – Illustration : discrminative power of $p_{\tau\ reco}$ and FD_τ on two of the dominant backgrounds.

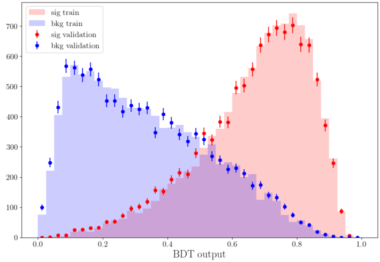

- Use of the MVA to perform the selection (cut at 0.5 on the BDT output).
- A pure signal sample is obtained on to the signal window.

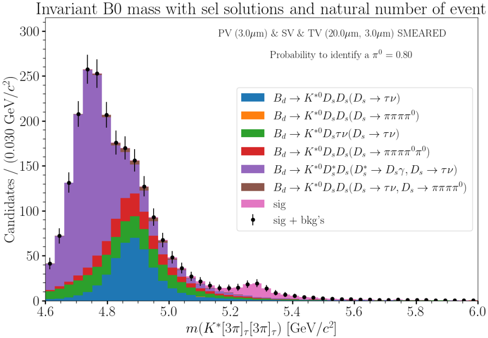

- Same selection applied to other vertex resolution emulations.
- Unbinned ML fit of the data with :
  - signal $\rightarrow$ double CB + a Gaussian,
  - background $\rightarrow$ two decreasing exponential.
- Baseline : fit of the simulated signal then fit of the signal and background rescaled together.
- Extraction of the signal yield N and the associated error σ_N.
- Plot of the naive precision σ_N/N of the BF measurement of $B^0 \rightarrow K^{*0}\tau\tau$ as function of the resolution [viii].

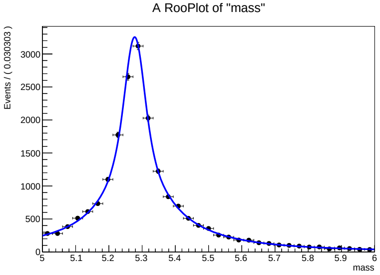

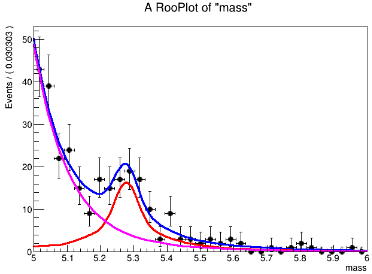

viii. **Points from other longitudinal resolutions in appendix.**

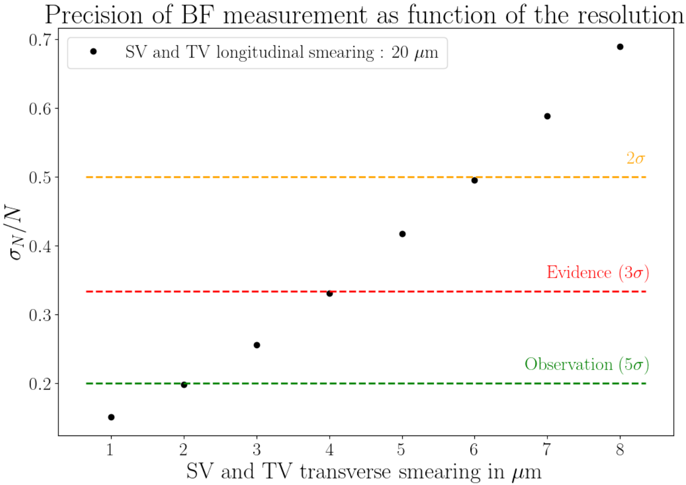

Figure – Precision on the BF measurement as function of the vertex resolution. Only 20μm of longitudinal resolution displayed, because this resolution has a weak impact. Evidence of $B^0 \to K^{*0}\tau\tau$ reach with a transverse vertex resolution of 4μm, observation reach with a 2μm resolution.

- Emulation of the vertex resolution performances in order to look for the feasibility of the search for $B^0 \to K^{*0}\tau\tau$ at FCC-*ee*.
- Observation possible with a transverse vertex resolution of 2μm.

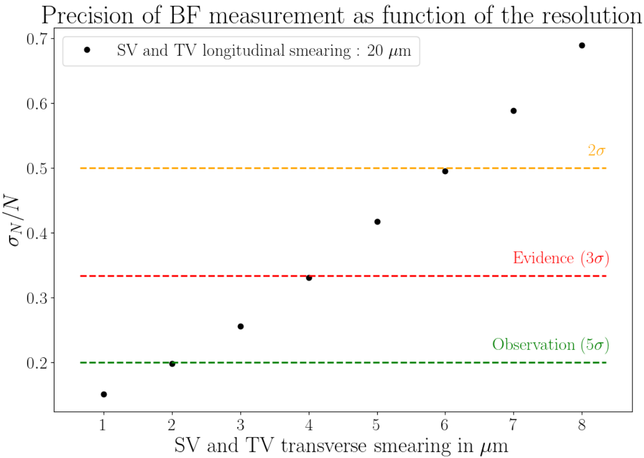

Last projection and outlook

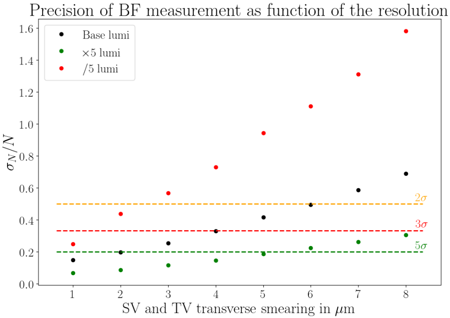

Figure – Precision on the BF measurement as function of the vertex resolution. Previous points are shown with the baseline luminosity and two other luminosity hypothesis are tested. Increasing the data taking period by a factor 5 bring us to a possible observation with a transverse vertex resolution of 5μm.

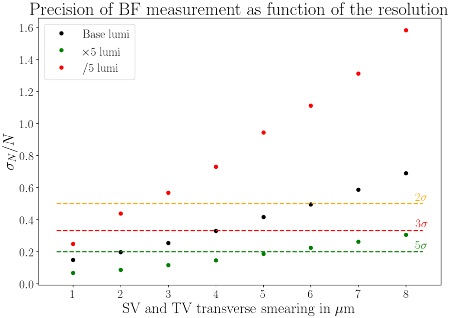

Figure – Precision on the BF measurement as function of the vertex resolution. Previous points are shown with the baseline luminosity and two other luminosity hypothesis are tested. Increasing the data taking period by a factor 5 bring us to a possible observation with a transverse vertex resolution of 5µm.

- Only the $\tau \to 3\pi\nu$ channel used here, method has to be build for other ones.
- First selection of $B^0 \to K^{*0}\tau\tau$ introduced ; first treatment of backgrounds $\to$ room for improvement.
- The conversion of the transverse size in term of single Impact Parameter performances has to be done.
- Calorimeter performance studies to back-up the hypothesis ε_{π^0}.

Thank for your attention !

To fully reconstruct the kinematics of the decay (B invariant-mass observable for instance) we need :

- Momentum of all final particles including not detected neutrinos.
- The decay lengths (6 constraints) together with the tau mass (2 constraints) can be used to determine the missing coordinates (6 degrees of freedom).
- We use energy-momentum conservation at tertiary (or τ decay) vertex with respect to τ direction [ix].

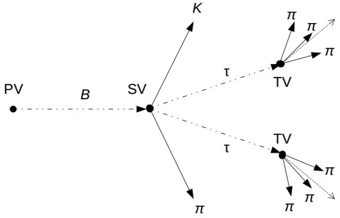

Figure – The dotted lines represent the non-reconstructed particles. The plain lines are the particles that can be reconstructed in the detector.

$$\begin{cases} p^{\perp}_{\nu_\tau} = -p^{\perp}_{\pi_t} \\ p^{\parallel}_{\nu_\tau} = \dfrac{((m^2_\tau - m^2_{\pi_t}) - 2p^{\perp,2}_{\pi_t})}{2(p^{\perp,2}_{\pi_t} + m^2_{\pi_t})}.p^{\parallel}_{\pi_t} \pm \dfrac{\sqrt{(m^2_\tau - m^2_{\pi_t})^2 - 4m^2_\tau p^{\perp,2}_{\pi_t}}}{2(p^{\perp,2}_{\pi_t} + m^2_{\pi_t})}.E_{\pi_t} \end{cases}$$

ix. Another way to do this computation is given by [9].

There is a quadratic ambiguity on each neutrino momentum !

$\rightarrow$ The ambiguities propagate to τ and B reconstructions

$\rightarrow$ 4 possibilities by taking all +/- combination for the two neutrinos

$\Rightarrow$ A selection rule is needed to choose the right possibility

$\longrightarrow$ From the energy-momentum conservation at the B decay vertex, we have a condition between the 2 taus and the K^* with respect to the B direction :

$$p_{\tau^+_-} = -\frac{\vec{p}^{\perp}_{K*}.\vec{e}_{\tau^+_-}}{1-(\vec{e}_{\tau^+_-}.\vec{e}_B)^2} - p_{\tau^-_+}.\frac{\vec{e}_{\tau^+_-}.\vec{e}_{\tau^-_+} - (\vec{e}_{\tau^+_-}.\vec{e}_B)(\vec{e}_{\tau^-_+}.\vec{e}_B)}{1-(\vec{e}_{\tau^+_-}.\vec{e}_B)^2}$$

The knowledge of the reconstruction efficiency allows us to compute the expected number of B^0 decays fully reconstructed at FCC-*ee* :

$$\mathcal{N}_{K^*\tau\tau\to K7\pi2\nu} = \mathcal{N}_Z.BR(Z \to b\bar{b}).2f_d.BR(K^*\tau\tau).BR(\tau \to \pi\pi\pi\nu)^2.BR(K^* \to K\pi).\epsilon_{reco}$$

Where :

- $\mathcal{N}_Z = 5 \times 10^{12}$ the expected number of Z produced,
- $BR(Z \to b\bar{b}) = 0.1512 \pm 0.0005$,
- $f_d = 0.407 \pm 0.007$ the hadronisation term,
- $BR(K^*\tau\tau) = 1.30 \times 10^{-7} \pm 10\%$ the SM predicted branching fraction,
- $BR(\tau \to \pi\pi\pi\nu) = 0.0931 \pm 0.0005$,
- $BR(K^* \to K\pi) = 0.69$,
- $\epsilon_{reco} = 0.3851 \pm 0.0007$ for a smearing $3\,\mu m/20\,\mu m$,

$$\Rightarrow \mathcal{N}_{K^*\tau\tau\to K7\pi2\nu} \approx 184 \pm 24.$$

Note : could be improved a bit by taking in addition other channels for τ : $\tau \to \pi\pi\pi\pi^0\nu$ for example $\to$ potential factor two.

Better simulations for $D_s \to \pi\pi\pi n\pi^0$

- Previously this decay has been generated in the Phase Space $\to$ a more accurate simulation of the decay is needed $\Rightarrow$ new samples which include η/ω (saturating the inclusive BF) intermediate states are in order.
- Replacement of the previous samples.
- $B^0 \to K^{*0} D_s D_s (D_s \to \pi\pi\pi\pi^0)$ is now $B^0 \to K^{*0} D_s D_s$ where $D_s \to \eta/\omega\pi$ and $\eta/\omega \to \pi\pi\pi^0$.
- $B^0 \to K^{*0} D_s D_s (D_s \to \pi\pi\pi\pi^0\pi^0)$ is now $B^0 \to K^{*0} D_s D_s$ where $D_s \to \eta/\omega\pi\pi^0$ and $\eta/\omega \to \pi\pi\pi^0$.

Data[x]	Reconstruction 20 − 3
$B^0 \to K^{*0}\tau\tau(\tau \to \pi\pi\pi\nu)$	0.38572 ± 0.00066
$B^0 \to K^{*0}D_sD_s(D_s \to \tau\nu)$	0.47272 ± 0.00040
$B^0 \to K^{*0}D_sD_s(D_s \to \pi\pi\pi\pi^0)$	0.01890 ± 0.00004
$B^0 \to K^{*0}D_sD_s(D_s \to \pi\pi\pi\pi^0, \tau\nu)$	0.16794 ± 0.00030
$B^0 \to K^{*0}D_sD_s(D_s \to \pi\pi\pi\pi^0\pi^0)$	0.49059 ± 0.00052
$B^0 \to K^{*0}D_s\tau\nu(D_s \to \tau\nu)$	0.42787 ± 0.00037
$B^0 \to K^{*0}D_s^*D_s(D_s^* \to D_s\gamma, D_s \to \tau\nu)$	0.48175 ± 0.00039

x. Warning the numbers here corresponds to the total reconstruction efficiency, not only to the component link to the neutrino reconstruction method as it was in last talks.

Data	$\varepsilon_{reco\ MC\ to\ RP}$
$B^0 \to K^{*0}\tau\tau(\tau \to \pi\pi\pi\nu)$	0.77174 ± 0.00133
$B^0 \to K^{*0}D_sD_s(D_s \to \tau\nu)$	0.78096 ± 0.00065
$B^0 \to K^{*0}D_sD_s(D_s \to \pi\pi\pi\pi^0)$	0.59227 ± 0.00110
$B^0 \to K^{*0}D_sD_s(D_s \to \pi\pi\pi\pi^0, \tau\nu)$	0.75827 ± 0.00135
$B^0 \to K^{*0}D_sD_s(D_s \to \pi\pi\pi\pi^0\pi^0)$	0.69084 ± 0.00103
$B^0 \to K^{*0}D_s\tau\nu(D_s \to \tau\nu)$	0.77075 ± 0.00066
$B^0 \to K^{*0}D_s^*D_s(D_s^* \to D_s\gamma, D_s \to \tau\nu)$	0.79386 ± 0.00064

Data	$\varepsilon_{reco\ \nu}\ 20-3$
$B^0 \to K^{*0}\tau\tau(\tau \to \pi\pi\pi\nu)$	0.49981 ± 0.00180
$B^0 \to K^{*0}D_sD_s(D_s \to \tau\nu)$	0.60530 ± 0.00087
$B^0 \to K^{*0}D_sD_s(D_s \to \pi\pi\pi\pi^0)$	0.03192 ± 0.00051
$B^0 \to K^{*0}D_sD_s(D_s \to \pi\pi\pi\pi^0, \tau\nu)$	0.22148 ± 0.00151
$B^0 \to K^{*0}D_sD_s(D_s \to \pi\pi\pi\pi^0\pi^0)$	0.71014 ± 0.00086
$B^0 \to K^{*0}D_s\tau\nu(D_s \to \tau\nu)$	0.55513 ± 0.00090
$B^0 \to K^{*0}D_s^*D_s(D_s^* \to D_s\gamma, D_s \to \tau\nu)$	0.60685 ± 0.00087

Distribution of π^0 momentum from $D_s \to 3\pi 2\pi^0$

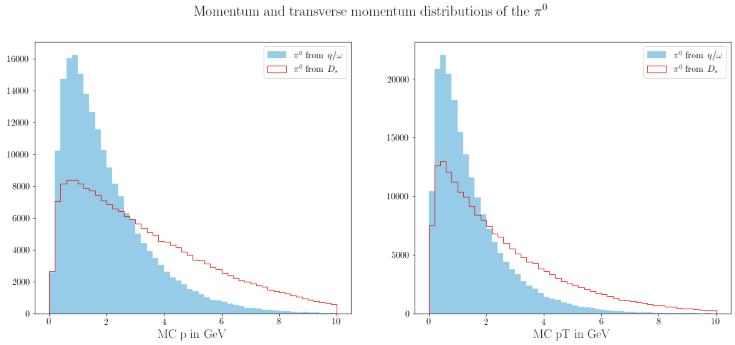

Figure – Distribution of π^0 momentum from $D_s \to 3\pi 2\pi^0$.

How $D_s \to \pi\pi\pi^0\pi^0$ mimic $\tau \to \pi\pi\pi\nu$

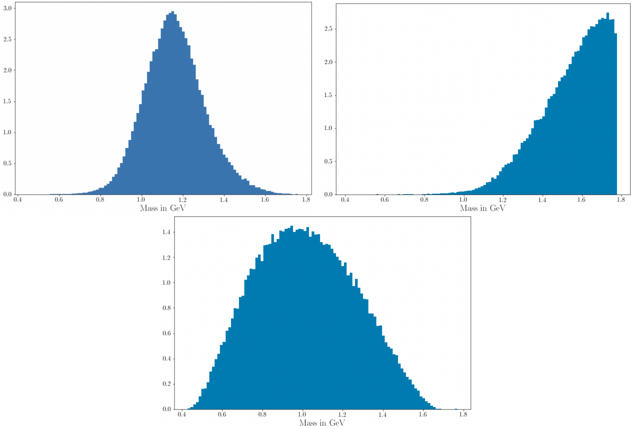

Figure – From top left to bottom, mass distribution (area normalized to 1) of the 3-pions system from $\tau \to \pi\pi\pi\nu$, $D_s \to \pi\pi\pi\pi^0$ and $D_s \to \pi\pi\pi\pi^0\pi^0$. $D_s \to \pi\pi\pi\pi^0$ candidates peaks clearly over the $\tau \to \pi\pi\pi\nu$ candidates, this is why so much events is killed by the reconstruction. Concerning $D_s \to \pi\pi\pi\pi^0\pi^0$ the second missing π^0 lead the distribution to peak close to the $\tau \to \pi\pi\pi\nu$ candidates, this is why the reconstruction doesn't kill it. $\tau \to \pi\pi\pi\nu$ is narrower than $D_s \to \pi\pi\pi\pi^0\pi^0$.

Reconstructed p_{tau} distribution signal vs backgrounds 20 − 3 configuration

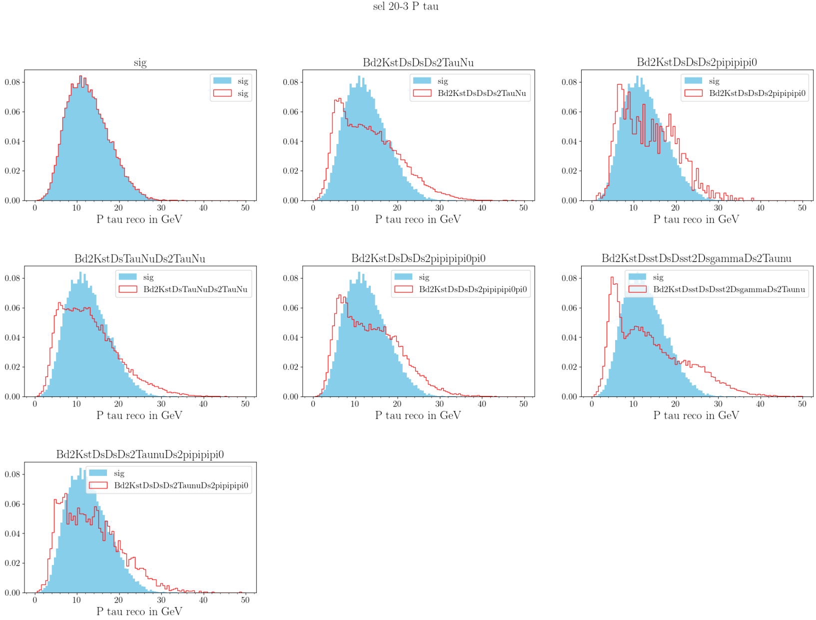

FD_{τ} distribution signal vs backgrounds 20 — 3 configuration

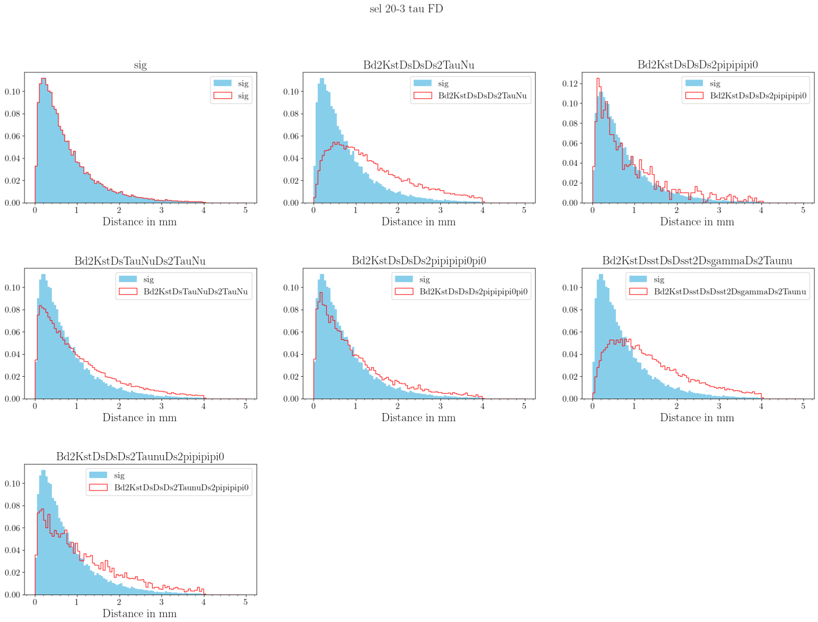

Precision of the measurement with other longitudinal resolutions.

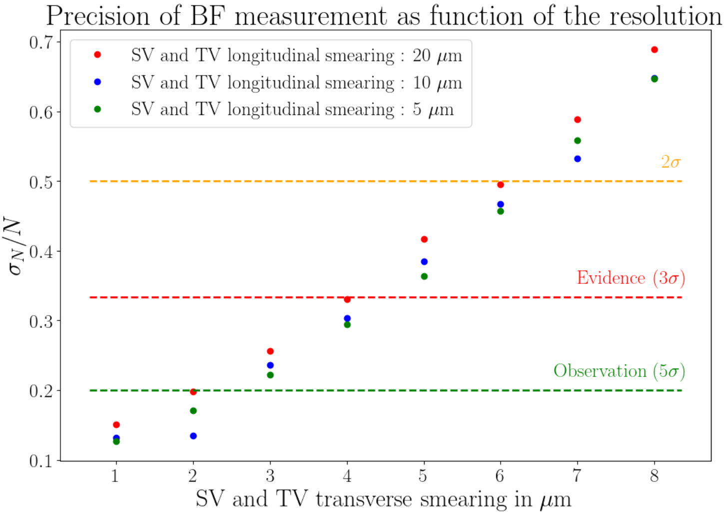

Figure – Precision on the BF measurement as function of the vertex resolution with 3 longitudinal configurations. Observed hierarchy issue comes from the interplay between the smearing of the vertexing and the fit model.

JF Kamenik, S Monteil, A Semkiv, and L Vale Silva.
Lepton polarization asymmetries in rare semi-tauonic $b \to s$ b→ s exclusive decays at fcc-ee.
The European Physical Journal C, 77(10) :1–19, 2017.

BABAR Collaboration et al.
Search for b+-> k+ tau (+) tau (-) at the babar experiment.
Physical Review Letters, 2017, vol. 118, num. 3, p. 031802, 2017.

Torbjörn Sjöstrand, Stefan Ask, Jesper R Christiansen, Richard Corke, Nishita Desai, Philip Ilten, Stephen Mrenna, Stefan Prestel, Christine O Rasmussen, and Peter Z Skands.
An introduction to pythia 8.2.
Computer physics communications, 191 :159–177, 2015.

Anders Ryd, David Lange, Natalia Kuznetsova, Sophie Versille, Marcello Rotondo, DP Kirkby, FK Wuerthwein, and A Ishikawa.
Evtgen : a monte carlo generator for b-physics.
BAD, 522 :v6, 2005.

J De Favereau, Christophe Delaere, Pavel Demin, Andrea Giammanco, Vincent Lemaitre, Alexandre Mertens, Michele Selvaggi, Delphes 3 Collaboration, et al.
Delphes 3 : a modular framework for fast simulation of a generic collider experiment.
Journal of High Energy Physics, 2014(2) :57, 2014.

CERN.
2nd fcc-france workshop, jan 20-21, 2021.
https:...Physics.pdf.

Juerg Beringer et al.
Particle data group.
Phys. Rev. D, 86(010001), 2012.

Tianqi Chen and Carlos Guestrin.
Xgboost : A scalable tree boosting system.
In *Proceedings of the 22nd acm sigkdd international conference on knowledge discovery and data mining*, pages 785–794, 2016.

Lingfeng Li and Tao Liu.
$b \rightarrow s\tau + \tau$- physics at future z factories.
Journal of High Energy Physics, 2021(6) :1–31, 2021.